

On the Vulnerability of Concept Erasure in Diffusion Models

Lucas Beerens^{*1} Alex D. Richardson^{*1,2} Kaicheng Zhang^{*1} Dongdong Chen³

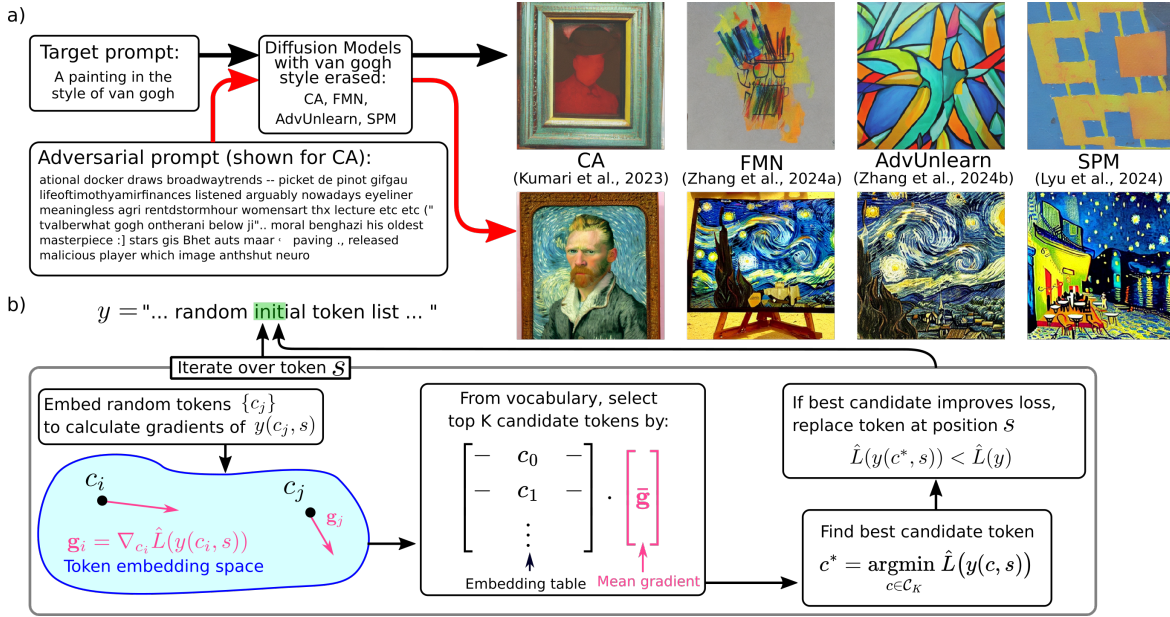


Figure 1. a) Examples of recalled behavior in various unlearned models, on van Gogh painting style. Shown is a specific adversarial prompt for CA (Kumari et al., 2023) b) Schematic of the update step in our RECORD Algorithm 1, where \hat{L} is our loss defined in Equation 5. We start with an initial prompt as a list of tokens, and iterate over these tokens. We randomly sample tokens to approximate the full gradient of the loss with respect to the all token embeddings. We then select the K candidate tokens from the full vocabulary that are most aligned with this gradient, and propose the token that minimizes the loss function. If the prompt with that new token achieves a better loss, we update it.

Abstract

The proliferation of text-to-image diffusion models has raised significant privacy and security concerns, particularly regarding the generation of copyrighted or harmful images. To address these issues, research on machine unlearning has developed various concept erasure methods, which aim to remove the effect of unwanted data

through post-hoc training. However, we show these erasure techniques are vulnerable, where images of supposedly erased concepts can still be generated using adversarially crafted prompts. We introduce **RECORD**, a coordinate-descent-based algorithm that discovers prompts capable of eliciting the generation of erased content. We demonstrate that RECORD significantly beats the attack success rate of current state-of-the-art attack methods. Furthermore, our findings reveal that models subjected to concept erasure are more susceptible to adversarial attacks than previously anticipated, highlighting the urgency for more robust unlearning approaches. We open source all our code at <https://github.com/LucasBeerens/RECORD>.

^{*}Equal contribution ¹School of Mathematics and Maxwell Institute, University of Edinburgh, Edinburgh, UK ²School of Physics and Astronomy, University of Edinburgh, Edinburgh, UK ³School of Mathematical and Computer Sciences, Heriot-Watt University, Edinburgh, UK. Correspondence to: Lucas Beerens <l.beerens@sms.ed.ac.uk>.

1. Introduction

Denosing diffusion models have become the standard for text-to-image generative models (Yang et al., 2024). The widespread proliferation and adoption of this technology has many ethical and societal impacts (Bendel, 2023), including the accessibility to production of harmful (violent, gory, pornographic, etc.) content and ease of copyright violation. Many large datasets include harmful or copyrighted data and, due to their size, it is difficult to clean them. Even so, retraining existing large models on cleaned datasets is expensive - especially if the definition of undesired output changes (such as changes in copyright law), requiring several re-trains. This has motivated the development of machine unlearning (or concept erasure) methods (Xu et al., 2023), where trained models are fine tuned to ‘forget’ small subsets of the training data. As many text-to-image generators are trained once on very large datasets that often include harmful material, and then hosted for the public to use, the importance of being able to cheaply and effectively ‘sanitize’ models by unlearning undesired behavior is clear.

Within the literature of machine unlearning, there are several standard goals (Xu et al., 2023). Models are fine tuned to unlearn specific objects (such as churches or parachutes); artistic styles (such as Van Gogh or Rembrandt); specific images (such as starry night by Van Gogh) and harmful concepts (such as nudity or gore). In this work, we verify the robustness of a wide range of unlearned models (Fan et al., 2023; Gandikota et al., 2023a; Kumari et al., 2023; Lyu et al., 2024; Wu et al., 2024; Wu & Harandi, 2024; Zhang et al., 2024a;b), on a range of tasks - van Gogh painting style, the concept of nudity, and objects (church, parachute, garbage truck). These are chosen as they are widespread tasks in the literature, with respectively unlearned model weights available. To address unlearning copyrighted data, it is sufficient to use a style or concept as a proxy. For example, if an artist requested that their work be removed from a training set, would unlearning the artist style be sufficient?

We find that all unlearned models are vulnerable to text based adversarial attacks (Figure 1a). This vulnerability also shows that ‘unlearning’ is misleading - model weights still contain information derived from undesirable images; and as such are still capable of producing undesired behavior. Instead, unlearning methods force models to suppress behaviors, under a range of standard prompt inputs, which is a form of model misalignment (Carlini et al., 2023). We believe this could have important consequences for copyright law - unlearning doesn’t remove information derived from copyrighted data from a model’s weights. We also compare the behaviors of different unlearned models to the stable diffusion (Rombach et al., 2022) they are based on, to highlight some inherent vulnerabilities of diffusion models,

and to gain insight into what concept erasure is actually doing.

Our contributions:

- We propose a novel algorithm RECORD to recall the unlearned behavior from any unlearned diffusion model. We find adversarial prompts that beat the current state-of-the-art by 10x on attack success rate.
- By optimizing prompt embeddings from many random initializations, we explore this space and demonstrate that near any random prompt embedding, there exist adversarially recalling prompt embeddings.
- We explore the behavior of recalled unlearned models by comparing semantically meaningful latent activations of their U-nets during inference. This suggests to us that unlearning algorithms do not erase concepts from the model weights, but instead deliberately misalign models to not generate specific concepts.

2. Background

2.1. Text-to-Image Diffusion Models

Diffusion Models are a class of generative model that generate images by learning to reverse the forward diffusion process. Starting with a Gaussian noise $x_T \sim \mathcal{N}(0, \mathbf{1})$, a trained denoiser, commonly U-Net (Ronneberger et al., 2015) or Vision Transformer (Dosovitskiy et al., 2020), iteratively denoises x_T over the timestep $t \in [0, T]$ until a clear image x_0 is reached. To perform text-to-image generation, the denoiser is trained conditioned on text embeddings $c = \mathcal{T}(y)$, where y is some natural language prompt, \mathcal{T} is a pre-trained text encoder, commonly CLIP (Radford et al., 2021) or BLIP (Li et al., 2022). By using datasets of text-image pairs, highly effective image denoisers can be trained that are conditioned on text input. In practice, many popular diffusion models (such as Stable Diffusion (Rombach et al., 2022)) perform the denoising on a latent space, where $z_t = \mathcal{E}(x_t)$, then z_t is iteratively denoised to z_0 and then decoded to $x_0 = \mathcal{D}(z_0)$. Here the latent space is defined by some image autoencoder, trained such that $x_0 \simeq \mathcal{D}(\mathcal{E}(x_0))$. To train a diffusion model, Gaussian noise ϵ is iteratively added to z_0 to reach z_t . The denoiser ϵ_θ can then be trained by optimizing

$$\underset{\theta}{\operatorname{argmin}} \mathbb{E}_{z \sim \mathcal{E}(x), t, \epsilon \sim \mathcal{N}(0, \mathbf{1}), c} \|\epsilon - \epsilon_\theta(z_t, t, c)\|_2^2, \quad (1)$$

where ϵ_θ is predicting the noise ϵ that takes z_{t-1} to z_t , effectively learning to reverse the Gaussian noise diffusion process.

2.2. Concept Erasure

The simplest and most effective way to prevent the generation of undesired content is to remove such images from the training dataset. However, this manual removal process is unfeasible and requires the model to be re-trained from scratch. Instead, much research effort focuses on model-editing-based approach, developing frameworks to finetune models in a post-hoc manner to remove or suppress undesired content while maintaining the quality of other generated images. Some prominent methods that we will adversarially recall from include: Erased Stable Diffusion (ESD) (Gandikota et al., 2023a), Concept Ablation (CA) (Kumari et al., 2023), EraseDiff (ED) (Wu et al., 2024), Forget-Me-Not (FMN) (Zhang et al., 2024a), Unified Concept Editing (UCE) (Gandikota et al., 2023b), ScissorHands (SH) (Wu & Harandi, 2024), Saliency Unlearning (SalUn) (Fan et al., 2023), Concept-SemiPermeable Membrane (SPM) (Lyu et al., 2024), and AdvUnlearn (Zhang et al., 2024b). Most of these methods (ESD, CA, ED, FMN, UCE, SH, SalUn, SPM) involve fine-tuning the denoising U-net of the diffusion model. The exception is AdvUnlearn, which fine tunes the text embedding network.

2.3. Prompt Tuning

Manipulating prompts to elicit specific behaviors from language models, also known as prompt tuning, is an important topic in Natural Language Processing research. Ebrahimi et al. (2018) introduced HotFlip, generating adversarial examples through minimal character-level flips guided by gradients. Extending this, Wallace et al. (2021) developed Universal Adversarial Triggers—input-agnostic token sequences optimized by using a first order Taylor-expansion around the current token to select candidate tokens for exact evaluation. Shin et al. (2020) presented AutoPrompt, which uses this algorithm to automatically generate prompts for various use cases. Addressing the lack of fluency in these prompts, Shi et al. (2022) introduced FluentPrompt, incorporating fluency constraints and using Langevin Dynamics combined with Projected Stochastic Gradient Descent, where projection is done onto the set of token embeddings.

Wen et al. (2023) developed PEZ, an algorithm inspired by FluentPrompt. It allows for prompt creation in both text-to-text and text-to-image applications. In text-to-image models, Gal et al. (2022) applied Textual Inversion, learning “pseudo-words” in the embedding space to capture specific visual concepts. Further advancements include GBDA (Guo et al., 2021), enabling gradient-based optimization over token distributions using the Gumbel-Softmax reparametrization (Jang et al., 2017) to stay on the probability simplex, and ARCA (Jones et al., 2023), optimizing discrete prompts via an improvement to AutoPrompt. ARCA will inspire our method.

2.4. Concept Restoration

Recently methods have been developed that aim to restore concepts intentionally unlearned from models by leveraging advanced optimization techniques inspired by prompt tuning. Concept Inversion (CI) (Pham et al., 2023) introduces a new token with a learnable embedding to represent the erased concept, optimized by minimizing reconstruction loss during denoising—directly applying Textual Inversion from prompt tuning to the concept restoration paradigm (Gal et al., 2022). Prompting Unlearned Diffusion Models (PUND) (Han et al., 2024) enhances this approach by iteratively erasing and searching for the concept by also updating model parameters, improving transferability across models.

Other methods focus on discrete token optimization. UnlearnDiffAtk(UD) (Zhang et al., 2023) performs optimization over token distributions, similar to GBDA (Guo et al., 2021), but utilizes projection onto the probability simplex instead of the Gumbel-Softmax reparametrization. Prompting4Debugging (P4D) (Chin et al., 2023) optimizes prompts in the embedding space and projects onto discrete embeddings, akin to the approach used in PEZ (Wen et al., 2023). Additionally, Ring-A-Bell (Tsai et al., 2023) constructs an empirical representation of the erased concept by averaging embedding differences from prompts with and without the concept, then employs a genetic algorithm to optimize the prompt.

These methods demonstrate that optimization techniques from prompt tuning—both in continuous embeddings and discrete token spaces—can be used for algorithms to circumvent concept unlearning.

3. Method

3.1. Motivation: Vulnerability of Machine Unlearning

Vulnerability Verifying that a model has truly unlearned a concept is challenging. We consider an unlearned model¹ $\epsilon_{\theta'}$ to be robust if it consistently fails to generate the erased content, even when subjected to *any* adversarial prompt. In this work we demonstrate that all unlearned models are not robust, rather they are vulnerable. We construct a loss function (Chin et al., 2023) that, when minimized, directly breaks this robustness definition:

$$L(y) = \mathbb{E}_{t, \mathbf{z}} \left[\left\| \epsilon_{\theta'}(\mathbf{z}_t, t, \mathcal{T}(y)) - \epsilon_{\theta}(\mathbf{z}_t, t, \mathcal{T}(y_{\text{target}})) \right\|_2^2 \right] \quad (2)$$

where \mathbf{z}_t is obtained through the forward diffusion process with $\mathbf{z}_0 \sim p_{\text{target}}$ coming from the target data distribution,

¹With ‘unlearned’ we mean a trained model that has been fine tuned to unlearn something, not an untrained model.

and y_{target} is the target prompt. See appendices A,B for more discussion on loss functions.

Latent spaces. To further understand the vulnerability of unlearned models, we explore their behavior in various latent spaces of interest. Firstly we explore how, during the iterative optimization to recall, our adversarial prompts move along trajectories in the prompt embedding space. By trying to sample this space, we gain considerable insight into the vulnerability of unlearning. We compare the difference in behavior between optimizing *tokens* or prompt *embeddings*, by either optimizing equation 2 for prompts y or optimizing:

$$\tilde{L}(c) = \mathbb{E}_{t, \mathbf{z}} \|\epsilon_{\theta'}(\mathbf{z}_t, t, c) - \epsilon_{\theta}(\mathbf{z}_t, t, c_{\text{target}})\|_2^2 \quad (3)$$

for embeddings c where c_{target} is the embedding of our target concept. Both optimization processes recall unlearned behavior, but they explore different regions of the input space, and therefor demonstrate different vulnerabilities. We also take inspiration from interpretability research (Ijishakin et al.; Surkov et al., 2024; Park et al., 2023) where the internal activations (especially near the bottleneck) of the denoising U-net provide semantically meaningful latent spaces. We compare trajectories in these spaces during inference, for a range of recalled unlearned models and baseline models.

3.2. RECORD

We introduce **RECORD** (Recalling Erased Concepts via Coordinate Descent), an algorithm for evaluating and challenging the robustness of concept erasure methods. RECORD searches for adversarial prompts that cause unlearned models to generate images containing erased concepts, thereby revealing any residual concept information retained after unlearning. Given an original model θ , an unlearned model θ' , and a target prompt y_{target} representing the erased concept, our goal is to find an adversarial prompt y^* that minimizes Equation 2. Let $L(y)$ denote this expectation for a prompt y with optimal prompt

$$y^* = \underset{y}{\operatorname{argmin}} L(y). \quad (4)$$

Since computing the exact expectation over all latents and timesteps is intractable, we approximate $L(y)$ by sampling batches:

$$\hat{L}(y, \mathcal{Z}) = \sum_{(\mathbf{z}_t, t) \in \mathcal{Z}} \left\| \epsilon_{\theta'}(\mathbf{z}_t, t, \mathcal{T}(y)) - \epsilon_{\theta}(\mathbf{z}_t, t, \mathcal{T}(y_{\text{target}})) \right\|_2^2, \quad (5)$$

where \mathcal{Z} is a set of noised images and their corresponding timesteps. We maintain a reference set \mathcal{R} of noised images and timesteps to consistently evaluate optimization progress. The key challenge in optimizing this objective

Algorithm 1 Pseudocode of RECORD.

```

#  $\theta'$ : original model;  $\theta$ : unlearned model
#  $y_{\text{target}}$ : target prompt
#  $J$ : gradient samples;  $K$ : candidates
#  $S$ : sequence length;  $N$ : passes
#  $R$ : reference set;  $E$ : embedding table

Random token sequence  $y$  of length  $S$ : # initialization
for n=1 to N: # load N passes
    # Shuffle
    Random permutation  $\pi$  of positions  $\{1, \dots, S\}$ 

    for s in  $\pi$ :
        # sample data
        Sample batch  $\mathcal{Z}$  of noise images and timesteps
        # candidate selection
        | Sample  $J$  random tokens  $\{c_j\}$ 
        | Compute gradients  $\mathbf{g}_j$  via (6)
        | Score all tokens: scores  $\leftarrow E \bar{\mathbf{g}}$ 
        | Select top  $K$  tokens  $\mathcal{C}$  based on scores

        # candidate evaluation
         $\hat{c}^* = \operatorname{argmin}_{c \in \mathcal{C}} \hat{L}(y(c, s), \mathcal{Z})$  # best candidate
        # coordinate descent
        if  $\hat{L}(y(\hat{c}^*, s), \mathcal{R}) < \hat{L}(y, \mathcal{R})$ :
            Update  $y \leftarrow y(\hat{c}^*, s)$ 

Return: optimized prompt  $y$  for recalling erased
concepts
    
```

lies in the discrete nature of the token sequence space and the non-differentiable mapping from tokens to embeddings. Standard gradient-based methods are not directly applicable. Instead, we employ coordinate descent, iteratively optimizing one token at a time while keeping others fixed.

RECORD begins by initializing a random token sequence $y = [y_1, \dots, y_S]$ of length S . To iteratively refine this sequence, we perform N passes over y . In each pass, we generate a random permutation of the token positions to mitigate positional bias during updates. For each position s in the permuted sequence, the algorithm samples a batch of K images $\mathbf{z}_0^{(n)}$ and corresponding timesteps $t^{(n,s)}$. Candidate tokens for position s are then selected using a gradient-based approximation method. These candidates are evaluated using a predefined objective function, and if any candidate yields an improvement according to the evaluation metric, y_s is updated. This iterative process continues for all positions in the permutation and repeats for N passes, progressively enhancing the token sequence over time. A pseudocode can be found in Algorithm 1.

To efficiently select candidate tokens at each position, we use an approximation strategy. We sample J random tokens and compute gradients with respect to their embeddings:

$$\mathbf{g}_j = \nabla_{c_j} \hat{L}(y(c_j, s), \mathcal{Z}(n, s)). \quad (6)$$

The average gradient $\bar{\mathbf{g}} = \frac{1}{J} \sum_{j=1}^J \mathbf{g}_j$ provides a linear approximation of how the loss changes with different token embeddings. By multiplying the embedding table E with $\bar{\mathbf{g}}$, we efficiently score all possible tokens and select the top C candidates for exact evaluation.

To ensure stable optimization in the discrete token space,

Table 1. Attack success rate (%) for models with the van Gogh style erased. Comparing the restoration methods P4D (Chin et al., 2023), UD (Zhang et al., 2023), and RECORD (ours).

Erased Concept	Restoration Method	Erasure Method					
		ESD Gandikota et al., (2023a)	FMN Zhang et al., (2024a)	AC Kumari et al., (2023)	SPM Lyu et al., (2024)	UCE Gandikota et al., (2023b)	AdvUnlearn Zhang et al., (2024b)
Van Gogh	No attack	3.4	17.6	32.2	45.4	52.8	0.8
	P4D	6.6	27.2	49.8	54.8	67.2	2.8
	UD	5.4	25.4	17.0	34.6	42.8	2.8
	RECORD	64.0	76.8	94.0	95.6	97.6	33.0

Table 2. Attack success rate (%) for models with the concepts Church, Garbage Truck, Parachute, and Nudity erased. Comparing the restoration methods P4D (Chin et al., 2023), UD (Zhang et al., 2023), and RECORD (ours).

Erased Concept	Restoration Method	Erasure Method					
		ED Wu et al., (2024)	ESD Gandikota et al., (2023a)	SalUn Fan et al., (2023)	SH Wu & Harandi, (2024)	SPM Lyu et al., (2024)	AdvUnlearn Zhang et al., (2024b)
Church	No attack	2.0	20.2	4.4	1.0	84.6	1.6
	P4D	16.0	24.6	28.8	3.4	51.6	7.0
	UD	2.6	4.8	5.4	4.4	22.8	1.4
	RECORD	61.2	75.2	71.4	8.6	92.2	57.0
Garbage Truck	No attack	20.4	6.2	9.0	9.2	28.4	0.2
	P4D	9.4	18.8	21.0	0.4	35.8	34.2
	UD	16.0	3.8	17.0	4.4	29.2	0.2
	RECORD	40.8	38.8	58.0	1.0	66.4	50.0
Parachute	No attack	3.8	0.8	1.2	2.2	29.8	0.2
	P4D	5.6	11.6	20.6	0.6	15.6	2.0
	UD	3.0	2.4	2.4	1.0	6.8	1.2
	RECORD	15.4	44.6	48.8	2.0	60.4	35.6
Nudity	No attack	7.0	49.2	1.8	2.0	49.6	38.4
	P4D	2.0	37.6	9.8	9.6	28.8	17.0
	UD	4.0	19.2	4.2	2.0	2.5	14.2
	RECORD	2.4	70.6	9.0	21.2	69.0	39.2

we employ a greedy update strategy. A candidate token \hat{c}^* is only accepted if it improves the loss on the reference set \mathcal{R} :

$$\hat{L}(y(\hat{c}^*, s), \mathcal{R}) < \hat{L}(y, \mathcal{R}). \quad (7)$$

Since each accepted token replacement strictly decreases the loss and the number of possible token sequences is finite, the algorithm is guaranteed to converge to a coordinate-wise local minimum.

4. Experiments

We compare RECORD against UD (Zhang et al., 2023) and P4D (Chin et al., 2023) on diffusion models unlearned with a large variety of methods (ESD (Gandikota et al., 2023a), ED (Wu et al., 2024), SH (Wu & Harandi, 2024), FMN (Zhang et al., 2024a), CA (Kumari et al., 2023), SPM (Lyu et al., 2024), SalUn (Fan et al., 2023), UCE (Gandikota et al., 2023b) and AdvUnlearn (Zhang et al., 2024b)). All the unlearned models we consider were unlearned from the baseline of a trained Stable Diffusion 1.4 (Rombach et al., 2022) text-to-image generator, which we just refer to as the ‘baseline’. The erased concepts include art style (Van Gogh), objects (church, garbage truck, parachute) and nudity, and the weights of the unlearned models are obtained from (Zhang et al., 2024b). We run each attack on one Nvidia H100 GPU. We also analyze the behavior of recalled

models to gain insight into how they are vulnerable. Note that not all unlearning techniques have been developed on all tasks.











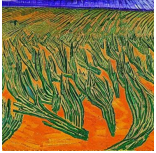






4.1. Evaluation metrics

It is common in the concept erasure literature to use a large variety of classifier models from different sources to evaluate the attack methods, as no one classifier is trained on all the erased concepts. However we alternatively use a single zero-shot diffusion classifier (Stable Diffusion v2.1) (Li et al., 2023; Clark & Jaini, 2023) to classify the generated image. The classification results are obtained by computing

$$y^* = \operatorname{argmin}_{y_i \in Y} \mathbb{E}_t \|\epsilon - \epsilon_\theta(z_t, t, \mathcal{T}(y_i))\|_2^2, \quad (8)$$

where $t \sim U(0, T)$, $Y = \{y_1, y_2, \dots, y_n\}$ is a set of n pre-specified classification classes, and the expectation is computed over 10 samples, which for our experiments is sufficient to provide good classification accuracies. For art style and object attacks, we build sets of 50 classes using prompt templates ‘a painting in the style of {artist_name}’ and ‘a photorealistic image of {object}’, where the artist names are randomly chosen from a list of famous painters, e.g. Leonardo Da Vinci, and object names are from the classification classes of YOLOv3 (Redmon & Farhadi, 2018). For nudity attacks, a set of 4 classes are built with the same

Table 3. Generated images of erased concepts using prompt attacks. Each image column of the same concept is generated using the same latent initialization. Models have unlearned the style of van Gogh paintings. Target prompt "a painting in the style of van Gogh".

Erased Concept	Restoration Method	Erasure Method						
		ESD Gandikota et al., (2023a)	FMN Zhang et al., (2024a)	AC Kumari et al., (2023)	SPM Lyu et al., (2024)	UCE Gandikota et al., (2023b)	AdvUnlearn Zhang et al., (2024b)	
Van Gogh	UnlearnDiff							
		P4D						
			RECORD					

template as the object attacks. For all attacks, we also additionally add one empty class, ' ', which empirically can help the classifier capture images that fall significantly outside the distributions of the specified classes. All results presented in this section use 500 images generated by the corresponding models and attacks. For all the various methods and models we report the Attack Success Rate (ASR) in percentage. This is calculated by dividing the number of images classified as the target by the total number of generated images.

4.2. Prompt Attacks

We evaluate RECORD by comparing it with UD (Zhang et al., 2023) and P4D (Chin et al., 2023). For a fair comparison, we give each method 64 tokens to optimize. Each method starts with a random prompt, except UD. Since UD optimizes on a token distribution, we give it a uniform distribution for all tokens except the first few that are initialized to be the target prompt. Without this type of initialization UD would not be able to get any significant performance.

For RECORD, we use $N = 20$ passes through the token list. We use batches of 1 image each. During the candidate selection, we make use of $J = 64$ samples. The chosen candidate set has size $K = 64$. These numbers are chosen to best use the available VRAM.

Each of the three methods are used to create 50 adversarial prompts. Every prompt is used to create 10 images for a total of 500 images per method to be used for ASR calculations.

Example images can be found in Table 3. Examples for different unlearned concepts can be found in Appendix C.

In Tables 1 and 2 we can see that RECORD outperforms both other methods consistently, except for a few minor exceptions. In particular, AdvUnlearn is quite resilient against P4D and UD with single digit ASR on most concepts, while RECORD is able to achieve an ASR of at least 33% for all concepts.

The low performance of all methods against SH can be explained by the findings by Zhang et al. (2024b) that SH degrades their image quality by a lot more than other methods to achieve this level of robustness.

4.3. Prompt embedding manifolds

To assess the vulnerability of unlearned U-nets, we sample the space of prompt embeddings to find where these models are vulnerable (Figure 3). We consider just ESD here, but find that all the other models behave the same. We also include the embedding optimization process on the baseline model for comparison. We perform a 2D isomap projection (Figure 3a) to visualize how trajectories of prompt embedding optimizations behave. We also include histograms of distance metrics between: initial and target (Figure 3b); optimized and target (Figure 3c); and initial and target positions (Figure 3d). Initial conditions are sampled 'close' to the target prompt of 'a painting in the style of van Gogh', by padding the target prompt with a random length of random characters. Initial conditions 'far' from the target were gen-

erated by uniformly randomly sampling characters. These classes of initial conditions separate into clusters of the latent space, but there is no discernible difference here between baseline and unlearned models. In any region of the prompt embedding space we sample, there exists a nearby adversarial prompt embedding, suggesting that unlearned models are vulnerable to small perturbations of prompt embeddings almost everywhere. Initial prompt embeddings of unlearned models that start near the target prompt embedding, move away from the target prompt embedding during embedding optimization. However this is less pronounced in the baseline model.

When RECORD optimizations are projected onto this same space (Figure 3), we see that they take much larger jumps than the continuous embedding optimization. We also find that, although initialized randomly, RECORD stays far away from the target prompt, despite taking large jumps over the space. This shows that unlearned models are also vulnerable to prompts that have little relation to the target prompt. We distinguish between ESD (Gandikota et al., 2023a) and AdvUnlearn (Zhang et al., 2024b) because AdvUnlearn has unlearned text encoder weights, whereas ESD has unlearned U-net weights. We find little difference in behavior.

4.4. Semantic Latents

To further explore the vulnerability of unlearned methods, we compare the behavior of recalled unlearned models and the baseline stable diffusion on the generation of van Gogh paintings. The bottleneck of the U-nets used for T2I diffusion models learn to represent a latent space with semantic meaning (Surkov et al., 2024; Park et al., 2023). We borrow the nomenclature from literature (Surkov et al., 2024) where ‘mid.0’ refers to the bottleneck of the U-net, and ‘down.2.1’ is the final downsampling block before this bottleneck.

By comparing the trajectories (during inference) of the activations in this semantic latent space, we can assess whether a recalled unlearned model is ‘close’ to the baseline with the target prompt 2. Most of the unlearning methods we compare work by modifying the weights near the U-net bottleneck, so inspecting the latent space defined by the activations at this region is reasonable. We find that recalled unlearned models have trajectories that are as ‘far away’ as unrelated prompts in this space from the baseline (Figure 2a-d). The fact that these trajectories still succeed in generating paintings in the style of van Gogh suggests that unlearning does not remove information from the U-net, but instead transforms how the U-net responds to text embeddings. Furthermore, we find that unlearned models with the target prompt produce trajectories much closer to the baseline-target prompt (Figure 2e-h), despite not rendering van Gogh paintings. This indicates that RECORD finds prompts that take far away trajectories in this semantic

latent space, but they still yield van Gogh paintings. This highlights the inherent complexity of such spaces, and suggests that unlearning requires a better understanding of how these models store semantic meaning.

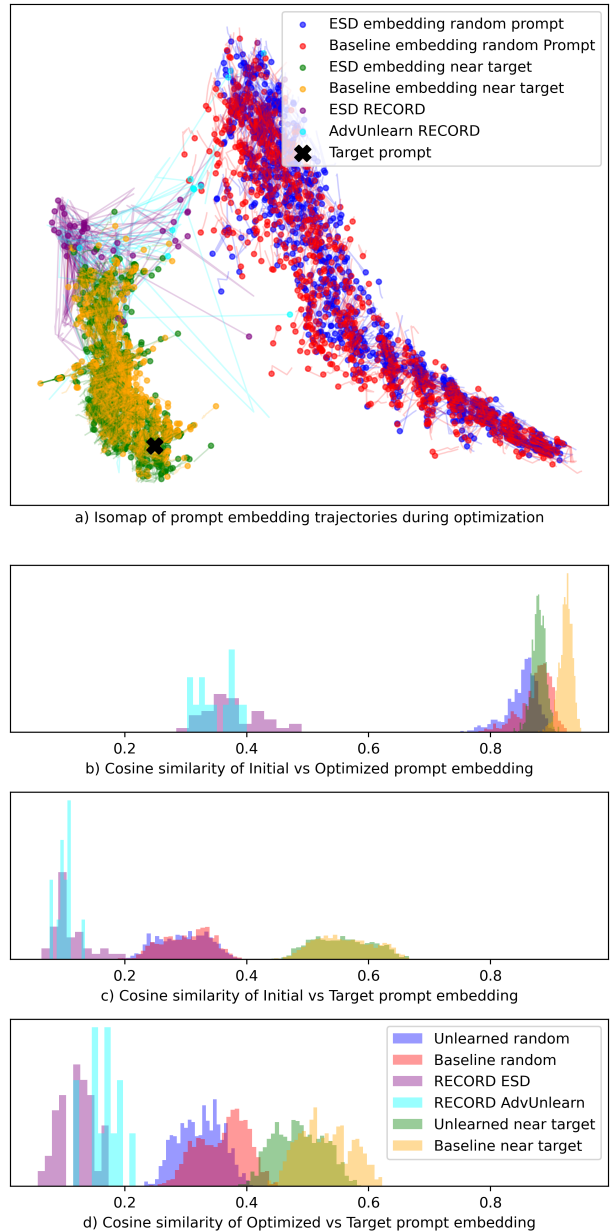


Figure 3. Behavior of prompt embedding vectors during RECORD and embedding optimization. a) Isomap projection of prompt embeddings for RECORD and embedding optimisation. b) Histograms of cosine similarities between initial and target embeddings. c) Histograms of cosine similarities between optimized and target embeddings. d) Histograms of cosine similarities between optimized and initial embeddings. All trajectories shown here successfully recall from the unlearned models

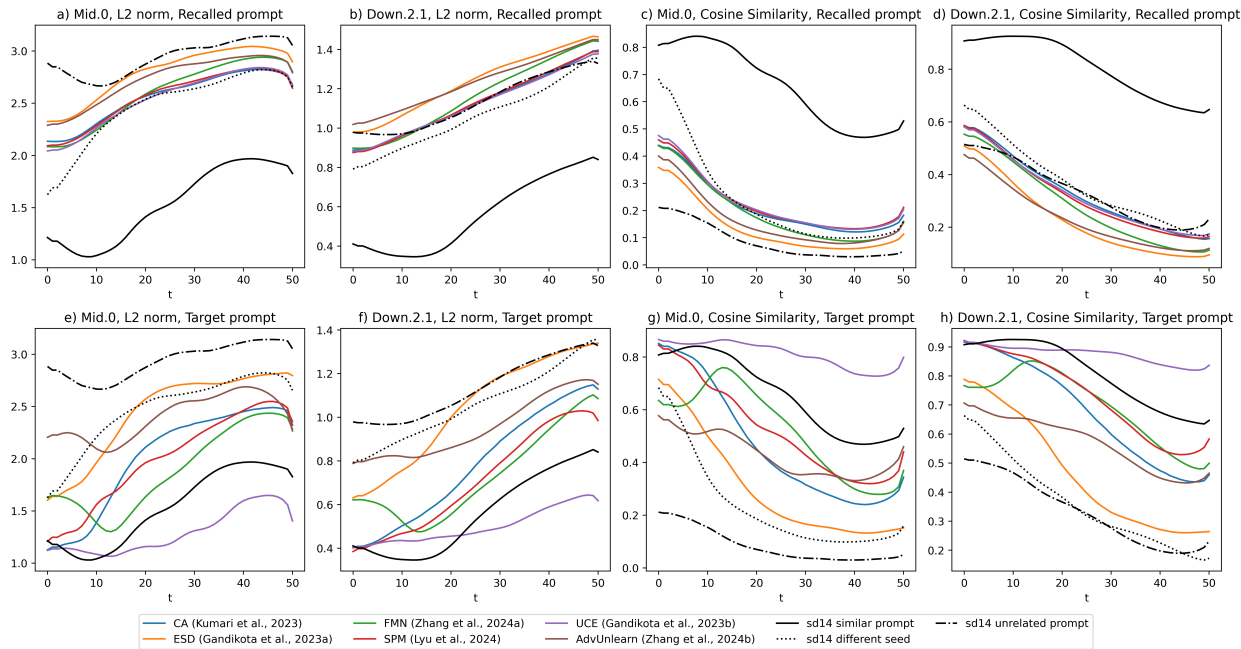


Figure 2. Comparison of activation trajectories during inference of RECORD unlearned (a-d) and unlearned with target prompt (e-h) to the trajectory of the baseline with target prompt. Mid.0 and Down.2.1 represent the bottleneck and final downsampling layers of the U-net. Target prompt: "a painting in the style of van gogh". We also compare the baseline with a semantically similar prompt "a painting of starry night by van gogh" and an unrelated prompt "a photorealistic image of a sports car", to gauge where semantically close or unrelated trajectories are expected to be. All generations use the same seed, except the baseline with 'different seed'. Unlearned trajectory distances are averaged over 20 successful adversarial prompts.

5. Discussion

We have demonstrated that existing machine unlearning methods do not erase the desired concept from diffusion models. We note that not all unlearning methods perform equally, in particular Scissorhands (Wu & Harandi, 2024) is the hardest to recall from, although it is still possible. As text-to-image generators proliferate and become ubiquitous, it is crucial that we understand how to minimize their misuse. Unfortunately the current paradigm of post-hoc unlearning harmful concepts from models trained on vast datasets is flawed.

Although we have demonstrated and explored how machine unlearning is currently vulnerable, we have not yet provided a solution. We suspect that robust unlearning would require far greater understanding of exactly how diffusion models store information, which in turn leads to problems in interpretability research. Work on semantic guidance during inference (Park et al., 2023; Surkov et al., 2024) could provide tools for isolating specific concepts in models, however there is no guarantee this would yield robust unlearning mechanisms.

Our methods have a few important weaknesses worth discussing. Firstly we obviously white-box access, which limits the utility of RECORD for recalling unlearned text-to-

image generators that one has black-box access to. Second is computational cost - with the limits of VRAM on Nvidia H100, we could only run RECORD with a batch size of 1.

6. Conclusions

Existing machine unlearning algorithms do not remove information from diffusion models. We have demonstrated, with a range of techniques, that these unlearned models can always be recalled to produce images of the so called erased concept. The behavior of recalled unlearned models when assessed during optimization of the recalling prompt/embedding, and during inference, suggests that these vulnerabilities are widespread and more serious than previously thought.

7. Acknowledgments

LB, AR, and KZ acknowledge support of MAC-MIGS CDT under EPSRC grant EP/S023291/1. This work was supported by the Edinburgh International Data Facility (EIDF) and the Data-Driven Innovation Programme at the University of Edinburgh. We thank Christos Christodoulopoulos for his useful discussions, and for his input to the Hackathon Workshop on Generative Modeling.

References

- Bendel, O. Image synthesis from an ethical perspective. *AI & SOCIETY*, September 2023. ISSN 1435-5655. doi: 10.1007/s00146-023-01780-4. URL <https://doi.org/10.1007/s00146-023-01780-4>.
- Carlini, N., Nasr, M., Choquette-Choo, C. A., Jagielski, M., Gao, I., Awadalla, A., Koh, P. W., Ippolito, D., Lee, K., Tramer, F., and Schmidt, L. Are aligned neural networks adversarially aligned? In *NeurIPS*, June 2023. doi: 10.48550/arXiv.2306.15447.
- Chin, Z.-Y., Jiang, C.-M., Huang, C.-C., Chen, P.-Y., and Chiu, W.-C. Prompting4Debugging: Red-teaming text-to-image diffusion models by finding problematic prompts. In *ICML*, September 2023. doi: 10.48550/arXiv.2309.06135.
- Clark, K. and Jaini, P. Text-to-image diffusion models are zero-shot classifiers. In *NeurIPS*, March 2023. doi: 10.48550/arXiv.2303.15233.
- Dosovitskiy, A., Beyer, L., Kolesnikov, A., Weissenborn, D., Zhai, X., Unterthiner, T., Dehghani, M., Minderer, M., Heigold, G., Gelly, S., Uszkoreit, J., and Houlsby, N. An Image is Worth 16x16 Words: Transformers for Image Recognition at Scale. October 2020. URL <https://openreview.net/forum?id=YicbFdNTTy>.
- Ebrahimi, J., Rao, A., Lowd, D., and Dou, D. HotFlip: White-box adversarial examples for text classification, May 2018.
- Fan, C., Liu, J., Zhang, Y., Wong, E., Wei, D., and Liu, S. SalUn: Empowering machine unlearning via gradient-based weight saliency in both image classification and generation. In *ICLR*, October 2023. doi: 10.48550/arXiv.2310.12508.
- Gal, R., Alaluf, Y., Atzmon, Y., Patashnik, O., Bermano, A. H., Chechik, G., and Cohen-Or, D. An image is worth one word: Personalizing text-to-image generation using textual inversion. In *ICLR*, August 2022. doi: 10.48550/arXiv.2208.01618.
- Gandikota, R., Materzynska, J., Fiotto-Kaufman, J., and Bau, D. Erasing concepts from diffusion models. In *ICCV*, March 2023a. doi: 10.1109/ICCV51070.2023.00230.
- Gandikota, R., Orgad, H., Belinkov, Y., Materzyńska, J., and Bau, D. Unified concept editing in diffusion models. In *IEEE Workshop/Winter Conference on Applications of Computer Vision*, pp. 5099–5108. arXiv, August 2023b. doi: 10.1109/WACV57701.2024.00503.
- Guo, C., Sablayrolles, A., Jégou, H., and Kiela, D. Gradient-based adversarial attacks against text transformers. In *EMNLP*, April 2021. doi: 10.18653/v1/2021.emnlp-main.464.
- Han, X., Yang, S., Wang, W., Li, Y., and Dong, J. Probing unlearned diffusion models: A transferable adversarial attack perspective, April 2024.
- Ijishakin, A., Ang, M. L., Baljer, L., Tan, D., Fry, H., Abdullaal, A., Lynch, A., and Cole, J. H-Space Sparse Autoencoders.
- Jang, E., Gu, S., and Poole, B. Categorical reparameterization with gumbel-softmax, August 2017.
- Jones, E., Dragan, A., Raghunathan, A., and Steinhardt, J. Automatically auditing large language models via discrete optimization. In *ICML*, March 2023. doi: 10.48550/arXiv.2303.04381.
- Kumari, N., Zhang, B., Wang, S.-Y., Shechtman, E., Zhang, R., and Zhu, J.-Y. Ablating concepts in text-to-image diffusion models. In *ICCV*, March 2023. doi: 10.1109/ICCV51070.2023.02074.
- Li, A. C., Prabhudesai, M., Duggal, S., Brown, E., and Pathak, D. Your diffusion model is secretly a zero-shot classifier. In *ICCV*, March 2023. doi: 10.1109/ICCV51070.2023.00210.
- Li, J., Li, D., Xiong, C., and Hoi, S. BLIP: Bootstrapping language-image pre-training for unified vision-language understanding and generation. In *ICML*, January 2022. doi: 10.48550/arXiv.2201.12086.
- Lyu, M., Yang, Y., Hong, H., Chen, H., Jin, X., He, Y., Xue, H., Han, J., and Ding, G. One-dimensional adapter to rule them all: Concepts, diffusion models and erasing applications. In *CVPR*, March 2024. doi: 10.1109/CVPR52733.2024.00722.
- Park, Y.-H., Kwon, M., Choi, J., Jo, J., and Uh, Y. Understanding the latent space of diffusion models through the lens of riemannian geometry. In *Proceedings of the 37th International Conference on Neural Information Processing Systems, NIPS '23*, Red Hook, NY, USA, 2023. Curran Associates Inc.
- Pham, M., Marshall, K. O., Cohen, N., Mittal, G., and Hegde, C. Circumventing concept erasure methods for text-to-image generative models. In *ICLR*, August 2023. doi: 10.48550/arXiv.2308.01508.
- Radford, A., Kim, J. W., Hallacy, C., Ramesh, A., Goh, G., Agarwal, S., Sastry, G., Askell, A., Mishkin, P., Clark, J., Krueger, G., and Sutskever, I. Learning transferable visual models from natural language supervision. In *ICML*, February 2021. doi: 10.48550/arXiv.2103.00020.

- Redmon, J. and Farhadi, A. YOLOv3: An Incremental Improvement, April 2018. 1145/3603620. URL <https://dl.acm.org/doi/10.1145/3603620>.
- Rombach, R., Blattmann, A., Lorenz, D., Esser, P., and Ommer, B. High-resolution image synthesis with latent diffusion models, April 2022.
- Ronneberger, O., Fischer, P., and Brox, T. U-Net: Convolutional Networks for Biomedical Image Segmentation. In Navab, N., Hornegger, J., Wells, W. M., and Frangi, A. F. (eds.), *Medical Image Computing and Computer-Assisted Intervention – MICCAI 2015*, pp. 234–241, Cham, 2015. Springer International Publishing. ISBN 978-3-319-24574-4. doi: 10.1007/978-3-319-24574-4_28.
- Shi, W., Han, X., Gonen, H., Holtzman, A., Tsvetkov, Y., and Zettlemoyer, L. Toward Human Readable Prompt Tuning: Kubrick’s *The Shining* is a good movie, and a good prompt too? In *EMNLP*, December 2022. doi: 10.48550/arXiv.2212.10539.
- Shin, T., Razeghi, Y., Logan Iv, R. L., Wallace, E., and Singh, S. AutoPrompt: Eliciting Knowledge from Language Models with Automatically Generated Prompts. In *EMNLP*, Online, 2020. doi: 10.18653/v1/2020.emnlp-main.346.
- Surkov, V., Wendler, C., Terekhov, M., Deschenaux, J., West, R., and Gulcehre, C. Unpacking SDXL turbo: Interpreting text-to-image models with sparse autoencoders, October 2024.
- Tsai, Y.-L., Hsu, C.-Y., Xie, C., Lin, C.-H., Chen, J.-Y., Li, B., Chen, P.-Y., Yu, C.-M., and Huang, C.-Y. Ring-a-bell! How reliable are concept removal methods for diffusion models? In *ICLR*, October 2023. doi: 10.48550/arXiv.2310.10012.
- Wallace, E., Feng, S., Kandpal, N., Gardner, M., and Singh, S. Universal adversarial triggers for attacking and analyzing NLP, January 2021.
- Wen, Y., Jain, N., Kirchenbauer, J., Goldblum, M., Geiping, J., and Goldstein, T. Hard prompts made easy: Gradient-based discrete optimization for prompt tuning and discovery. In *NeurIPS*, February 2023. doi: 10.48550/arXiv.2302.03668.
- Wu, J. and Harandi, M. Scissorhands: Scrub data influence via connection sensitivity in networks. In *ECCV*, January 2024. doi: 10.48550/arXiv.2401.06187.
- Wu, J., Le, T., Hayat, M., and Harandi, M. EraseDiff: Erasing data influence in diffusion models, July 2024.
- Xu, H., Zhu, T., Zhang, L., Zhou, W., and Yu, P. S. Machine Unlearning: A Survey. *ACM Comput. Surv.*, 56(1):9:1–9:36, August 2023. ISSN 0360-0300. doi: 10.1145/3603620.
- Yang, L., Zhang, Z., Song, Y., Hong, S., Xu, R., Zhao, Y., Zhang, W., Cui, B., and Yang, M. H. Diffusion Models: A Comprehensive Survey of Methods and Applications. *ACM Computing Surveys*, 56(4), April 2024. ISSN 0360-0300. doi: 10.1145/3626235. URL <http://www.scopus.com/inward/record.url?scp=85180157786&partnerID=8YFLogxK>.
- Zhang, G., Wang, K., Xu, X., Wang, Z., and Shi, H. Forget-me-not: Learning to forget in text-to-image diffusion models. In *CVPR*, Seattle, WA, USA, June 2024a. ISBN 979-8-3503-6547-4. doi: 10.1109/CVPRW63382.2024.00182.
- Zhang, Y., Jia, J., Chen, X., Chen, A., Zhang, Y., Liu, J., Ding, K., and Liu, S. To generate or not? Safety-driven unlearned diffusion models are still easy to generate unsafe images ... For now. In *ECCV*, October 2023. doi: 10.48550/arXiv.2310.11868.
- Zhang, Y., Chen, X., Jia, J., Zhang, Y., Fan, C., Liu, J., Hong, M., Ding, K., and Liu, S. Defensive unlearning with adversarial training for robust concept erasure in diffusion models, May 2024b.

A. Choice of loss function

Preliminary. We consider two loss functions from literature (Pham et al., 2023; Zhang et al., 2023; Chin et al., 2023), that when minimized would find such an adversarial prompt that recalls from unlearned models:

$$L_1(y) = \mathbb{E}_{t, \mathbf{z}} \left[\|\epsilon_{\theta'}(\mathbf{z}_t, t, \mathcal{T}(y)) - \epsilon\|_2^2 \right] \quad (9)$$

$$L_2(y) = \mathbb{E}_{t, \mathbf{z}} \left[\|\epsilon_{\theta'}(\mathbf{z}_t, t, \mathcal{T}(y)) - \epsilon_{\theta}(\mathbf{z}_t, t, \mathcal{T}(y_{\text{target}}))\|_2^2 \right] \quad (10)$$

where \mathbf{z}_t is obtained through the forward diffusion process with $\mathbf{z}_0 \sim p_{\text{target}}$ coming from the target data distribution, and y_{target} is the target prompt. L_1 (Pham et al., 2023) and L_2 (Chin et al., 2023) are minimized by prompts y that match the unlearned denoiser prediction respectively to: the true noise from the forward diffusion sequence \mathbf{z}_t ; and the predicted noise by the baseline denoiser with the target prompt. The main difference in behavior when optimizing both L_1 and L_2 derives from the imperfections of the baseline model - predictions of ϵ_{θ} don't perfectly match ϵ . We note that minimizing L_2 should find y that more accurately matches the behavior of the baseline model, including its imperfections.

Prompt embedding attacks. To compare both our loss functions, we first consider the simpler proxy problem of optimizing directly over prompt embeddings rather than prompts:

$$\tilde{L}_1(c) = \mathbb{E}_{t, \mathbf{z}} \|\epsilon_{\theta'}(\mathbf{z}_t, t, c) - \epsilon\|_2^2 \quad (11)$$

$$\tilde{L}_2(c) = \mathbb{E}_{t, \mathbf{z}} \|\epsilon_{\theta'}(\mathbf{z}_t, t, c) - \epsilon_{\theta}(\mathbf{z}_t, t, c_{\text{target}})\|_2^2. \quad (12)$$

As everything is continuous, the optimization is fairly straightforward.

B. Embedding Attacks

Before we demonstrate the prompt attacks, we explore prompt embedding attacks to compare our loss functions (Equations 9 and 10). We optimize on the continuous proxies (Equations 11 and 12), where Embed attack 1 and 2 minimize both \tilde{L}_1 and \tilde{L}_2 respectively. We use NAdam optimizer and iterate over a training set of 100 images 50 times, with a constant learning rate of 0.1 and a batch size of 16. The training set is generated by the original diffusion model using the target prompt. The two methods were used to create 500 adversarial prompt embeddings each. One image per prompt was created using the corresponding unlearned model.

The results are shown in Table 4. We notice that, when the classifier has a high accuracy in classifying the image from the original model, RECORD-embed works marginally better than the baseline. When the classification accuracy is already low on the original model, the difference between the two objectives becomes less obvious. This is because, when the original model can generate more ‘accurate’ images in the perspective of the classifier, its output can also act as a more informative surrogate to aid the attack process.

Additionally, when performing text embedding attacks on AdvUnlearn, which modifies only the text encoder rather than the U-Net, the problem in this case collapses to ‘finding a text embedding that can elicit the original diffusion model to generate the target concept’. Such text embedding is guaranteed to exist, and it is thus interesting to observe that in this seemingly easier setting, the attack success rate is not necessarily higher than other U-net-based concept erasure methods.

C. Example Images

Included here are example outputs of our and various other recalling methods, for a range of tasks and unlearned models.

D. RECORD with less tokens

In order to see the effect of the token count, we used RECORD with 16 and 32 tokens. The results can be found in Tables 10 and 11.

Table 4. The classification accuracy and the attack success rate of the embedding attacks for art style, object and nudity attacks.

		Baseline	Erasure Method					
			ESD Gandikota et al., (2023a)	FMN Zhang et al., (2024a)	AC Kumari et al., (2023)	SPM Lyu et al., (2024)	UCE Gandikota et al., (2023b)	AdvUnlearn Zhang et al., (2024b)
Van Gogh style	No attack	99.4	3.4	17.6	32.2	45.4	52.8	0.8
	Embed attack 1		99.8	99.8	99.4	100.0	91.4	92.8
	Embed attack 2		99.8	99.8	100.0	99.4	98.4	99.0

		Baseline	Erasure Method					
			ESD Gandikota et al., (2023a)	ED Wu et al., (2024)	SH Wu & Harandi, (2024)	SPM Lyu et al., (2024)	SalUn Fan et al., (2023)	AdvUnlearn Zhang et al., (2024b)
Church	No attack	98.8	20.2	4.4	1.0	84.6	2.0	1.6
	Embed attack 1		95.6	99.4	22.8	98.0	99.4	96.6
	Embed attack 2		100.0	100.0	64.6	99.8	100.0	100.0
Garbage Truck	No attack	93.4	6.2	20.4	9.2	28.4	9.0	0.2
	Embed attack 1		98.0	98.4	18.0	98.0	99.6	96.2
	Embed attack 2		98.8	100.0	3.8	99.6	100.0	92.4
Parachute	No attack	84.0	0.8	3.8	2.2	29.8	1.2	0.2
	Embed attack 1		91.2	89.6	4.8	73.6	63.0	46.6
	Embed attack 2		99.4	93.8	1.2	46.6	61.6	44.8

		Baseline	Erasure Method					
			ESD Gandikota et al., (2023a)	SH Wu & Harandi, (2024)	SPM Lyu et al., (2024)	SalUn Fan et al., (2023)	UCE Gandikota et al., (2023b)	AdvUnlearn Zhang et al., (2024b)
Nudity	No attack	87.6	49.2	2.0	49.6	1.8	41.8	38.4
	Embed attack 1		98.4	83.0	99.6	99.4	96.8	98.6
	Embed attack 2		98.2	87.6	98.6	99.8	98.8	96.8

Table 5. Generated images of erased concepts using embedding attacks. Each image column of the same concept is generated using the same latent initialization. Models have unlearned the style of van gogh paintings. Target prompt "a painting in the style of van gogh"






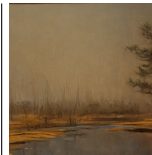



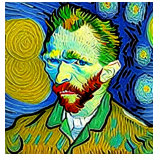
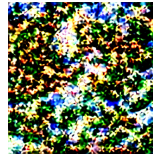





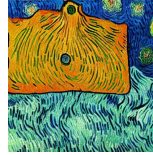

Erased Concept	Erasure Method						
	ESD Gandikota et al., (2023a)	FMN Zhang et al., (2024a)	AC Kumari et al., (2023)	SPM Lyu et al., (2024)	UCE Gandikota et al., (2023b)	AdvUnlearn Zhang et al., (2024b)	
Van Gogh	No attack						
	Embed attack 1						
	Embed attack 2						

Table 6. Generated images of erased concepts using embedding attacks. Each image column of the same concept is generated using the same latent initialization. Models have unlearned the concept of nudity. Target prompt asked for nudity.

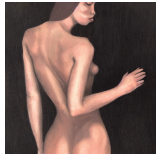
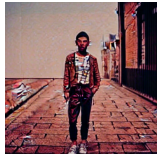




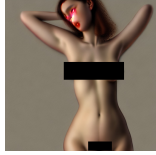

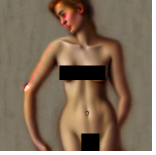
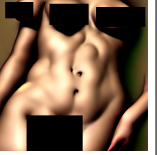
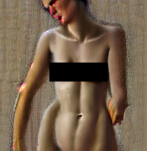
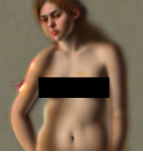
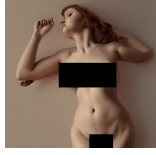
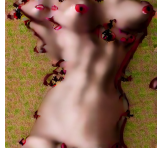
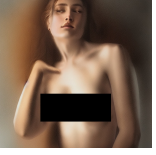
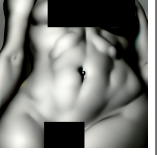
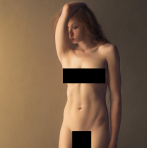










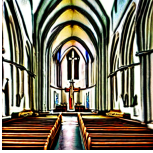


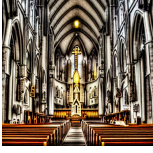





























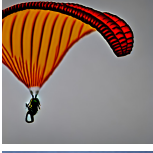
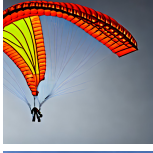

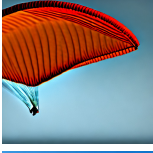




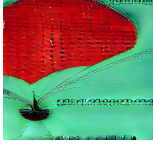



Erased Concept		Erasure Method					
		ESD Gandikota et al., (2023a)	SH Wu & Harandi, (2024)	SPM Lyu et al., (2024)	SalUn Fan et al., (2023)	UCE Gandikota et al., (2023b)	AdvUnlearn Zhang et al., (2024b)
Nudity	No attack						
	Embed attack 1						
	Embed attack 2						

Table 7. The generated images of erased concepts using embedding attacks. Each image column of the same concept is generated using the same latent initialization. Target prompt "a photorealistic image of *object*"

Erased Concept		Erasure Method					
		ESD Gandikota et al., (2023a)	ED Wu et al., (2024)	SH Wu & Harandi, (2024)	SPM Lyu et al., (2024)	SalUn Fan et al., (2023)	AdvUnlearn Zhang et al., (2024b)
Church	No attack						
	Embed attack 1						
	Embed attack 2						
	No attack						
	Embed attack 1						
	Embed attack 2						
Parachute	No attack						
	Embed attack 1						
	Embed attack 2						

On the Vulnerability of Concept Erasure in Diffusion Models

Table 8. The generated images of erased concepts using prompt attacks. Each image column of the same concept is generated using the same latent initialization. Target prompt "a photorealistic image of *object*"

Erased Concept		Erasure Method					
		ESD Gandikota et al., (2023a)	ED Wu et al., (2024)	SH Wu & Harandi, (2024)	SPM Lyu et al., (2024)	SalUn Fan et al., (2023)	AdvUnlearn Zhang et al., (2024b)
Church	UnlearnDiff						
	P4D						
	RECORD						
Garbage Truck	UnlearnDiff						
	P4D						
	RECORD						
Parachute	UnlearnDiff						
	P4D						
	RECORD						

On the Vulnerability of Concept Erasure in Diffusion Models

Table 9. The generated images of erased concepts using prompt attacks. Each image column of the same concept is generated using the same latent initialization. Target prompt asked for nudity.

Erased Concept		Erasure Method					
		ESD Gandikota et al., (2023a)	ED Wu et al., (2024)	SH Wu & Harandi, (2024)	SPM Lyu et al., (2024)	SalUn Fan et al., (2023)	AdvUnlearn Zhang et al., (2024b)
Nudity	UnlearnDiff						
	P4D						
	RECORD						

Table 10. Attack success rate (%) for models with the van Gogh style erased. Comparing RECORD with different allowed prompt lengths in terms of tokens.

Erased Concept	Prompt Length	Erasure Method					
		ESD Gandikota et al., (2023a)	FMN Zhang et al., (2024a)	AC Kumari et al., (2023)	SPM Lyu et al., (2024)	UCE Gandikota et al., (2023b)	AdvUnlearn Zhang et al., (2024b)
Van Gogh	16	26.2	53.8	89.6	85.6	94.2	13.6
	32	40.0	69.6	92.4	91.8	95.4	29.4
	64	64.0	76.8	94.0	95.6	97.6	33.0

Table 11. Attack success rate (%) for models with the concepts Church, Garbage Truck, Parachute, and Nudity erased. Comparing RECORD with different allowed prompt lengths in terms of tokens

Unlearned Concept	Prompt Length	Erasure Method					
		ED Wu et al., (2024)	ESD Gandikota et al., (2023a)	SalUn Fan et al., (2023)	SH Wu & Harandi, (2024)	SPM Lyu et al., (2024)	AdvUnlearn Zhang et al., (2024b)
Church	16	34.8	58.0	52.8	4.6	89.4	42.4
	32	43.6	67.0	66.6	5.4	94.8	55.6
	64	61.2	75.2	71.4	8.6	92.2	57.0
Garbage Truck	16	18.8	26.2	43.0	1.6	69.0	63.8
	32	34.0	33.8	60.4	1.0	72.0	59.6
	64	40.8	38.8	58.0	1.0	66.4	50.0
Parachute	16	6.0	31.0	32.8	2.0	45.8	17.2
	32	10.0	36.6	35.4	1.0	55.8	26.2
	64	15.4	44.6	48.8	2.0	60.4	35.6
Nudity	16	3.6	62.2	5.2	23.6	54.8	48.4
	32	2.2	65.0	6.6	22.0	65.8	51.6
	64	2.4	70.6	9.0	21.2	69.0	39.2